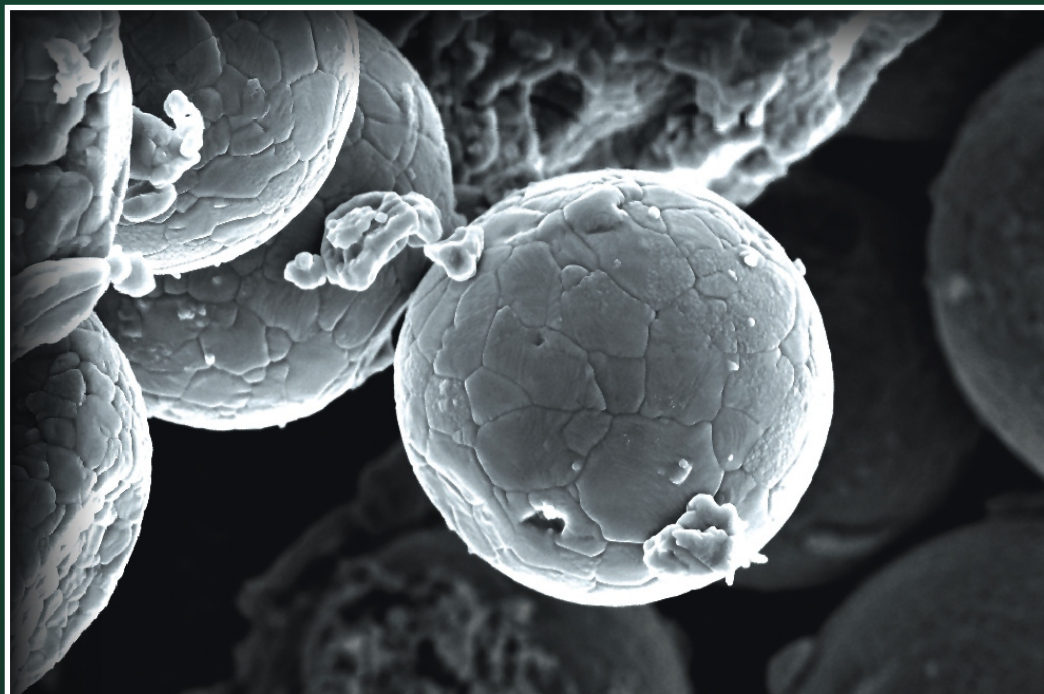


# MATERIAŁY ELEKTRONICZNE

## ELECTRONIC MATERIALS

PL ISSN 0209-0058



3

Vol. 44  
2016

M. Winkowska, L. Lipińska,  
T. Strachowski, M. Wasułkiewicz

Optimization of synthesis of single phase  
nanostructured  $\text{LiFePO}_4$  materials

4

M. Wójcik, J. Gaca, P. Caban,  
A. Turos

HRXRD study of  $\text{ZnO}$  single crystals bombarded  
with Ar ions

9

E. Brzozowski, B. Stańczyk,  
K. Przyborowska, A. Kozłowski

Resonator with transverse surface wave on lithium  
tantalate crystal for applications in viscosity  
and temperature sensors

17



INSTYTUT TECHNOLOGII MATERIAŁÓW ELEKTRONICZNYCH  
INSTITUTE OF ELECTRONIC MATERIALS TECHNOLOGY

<http://rcin.org.pl>



**INSTYTUT TECHNOLOGII  
MATERIAŁÓW ELEKTRONICZNYCH  
ul. Wólczyńska 133, 01-919 Warszawa**

**Z-ca Red. Naczelnego**

**tel.: (+48 22) 639 58 85**

**e-mail: Katarzyna.Pietrzak@itme.edu.pl**

**Dział Informacji Naukowej**

**i Technicznej**

**tel.: (+48 22) 639 55 29**

**e-mail: ointe@itme.edu.pl**

**www.itme.edu.pl**

Instytut Technologii Materiałów Elektronicznych wydaje dwa czasopisma naukowe, których tematyka dotyczy inżynierii materiałowej, elektroniki i fizyki ciała stałego, a w szczególności technologii otrzymywania nowoczesnych materiałów, ich obróbki, miernictwa oraz wykorzystania dla potrzeb elektroniki i innych dziedzin gospodarki:

- **Materiały Elektroniczne** – zawierające artykuły problemowe, teksty wystąpień pracowników ITME na konferencjach i Biuletyn PTWK,
  - **Prace ITME** – zawierające monografie, rozprawy doktorskie i habilitacyjne
- oraz
- stale aktualizowane katalogi i karty katalogowe technologii, materiałów, wyrobów i usług oferowanych przez Instytut i opartych o wyniki prowadzonych prac badawczych, opisy nowych wyrobów, metod i aparatury

Informacje można uzyskać:

**Promocja i Marketing tel.: (48 22) 639 58 32**

**e-mail: itme@itme.edu.pl**

INSTYTUT TECHNOLOGII MATERIAŁÓW ELEKTRONICZNYCH

**MATERIAŁY  
ELEKTRONICZNE**  
**ELECTRONIC MATERIALS**  
**KWARTALNIK**

**T. 44, Nr 3, 2016**  
**Vol. 44, No. 3, 2016**

Wydanie publikacji dofinansowane jest przez  
Ministerstwo Nauki i Szkolnictwa Wyższego

WARSZAWA ITME 2016

## KOLEGIUM REDAKCYJNE

**Z-ca Red. Naczelnego**  
dr hab. inż. Katarzyna PIETRZAK, prof. ITME

**Redaktorzy tematyczni:**  
prof. dr hab. inż. Andrzej JELEŃSKI  
dr hab. inż. Paweł KAMIŃSKI, prof. ITME  
dr hab. Dorota PAWLAK, prof. ITME  
dr inż. Włodzimierz STRUPIŃSKI  
prof. dr hab. inż. Andrzej TUROS

**Rada programowa:**  
prof. dr hab. Jacek BARANOWSKI  
prof. dr hab. inż. Zbigniew BIELECKI  
prof. dr hab. Marek GODEŁWSKI  
prof. dr hab. Maria KAMIŃSKA  
dr hab. inż. Jarosław MIZERA, prof. PW  
prof. dr hab. inż. Antoni ROGALSKI

**Sekretarz redakcji:**  
mgr Anna WAGA

**Redaktorzy językowi:**  
mgr Maria SIWIK - GRUŻEWSKA  
mgr Krystyna SOSNOWSKA

**Redaktor techniczny:**  
mgr Szymon PLASOTA

## ADRES REDAKCJI

**Instytut Technologii Materiałów Elektronicznych**  
ul. Wólczyńska 133, 01-919 Warszawa,  
e-mail: ointe@itme.edu.pl;  
www: matelektron.itme.edu.pl

## KONTAKT

**Z-ca Red. Naczelnego:**  
tel.: (22) 639 58 85  
**sekretarz redakcji:** (22) 639 55 29

**PL ISSN 0209 - 0058**

**Kwartalnik notowany na liście czasopism naukowych**  
**Ministerstwa Nauki i Szkolnictwa Wyższego**  
7 pkt. - wg komunikatu MNiSW.

**Opublikowane artykuły są indeksowane w bazach**  
**danych:** BazTech, CAS - Chemical Abstracts oraz Index Copernicus

**Publikowane artykuły mające charakter naukowy są**  
**recenzowane przez samodzielnego pracowników naukowych.**

**Wersja papierowa jest wersją pierwotną.**  
**Kwartalnik publikowany jest w otwartym dostępie.**  
**Nakład:** 200 egz.

**Na okładce:** ditlenek tytanu - tlenek tytanu (IV) -  $TiO_2$  otrzymany zmodyfikowaną metodą zol-żel.

**Autor próbki:** dr inż. Monika Michalska  
**Autor zdjęcia:** mgr Magdalena Romaniec

## SPIS TREŚCI - CONTENTS

Optimization of synthesis of single phase nanostructured $LiFePO_4$ materials	M. Winkowska, L. Lipińska, T. Strachowski, M. Wasiucionek	4
Optymalizacja procesu syntezy jednofazowych materiałów $LiFePO_4$ o nanometrycznych rozmiarach ziaren		
HRXRD study of ZnO single crystals bombarded with Ar ions	M. Wójcik, J. Gaca, P. Caban, A. Turos	9
Badanie metodami wysokotorzdziczej dyfraktometrii rentgenowskiej monokryształów ZnO bombardowanych jonami Ar		
Resonator with transverse surface wave on lithium tantalate crystal for applications in viscosity and temperature sensors	E. Brzozowski, B. Stańczyk, K. Przyborowska, A. Kozłowski	17
Rezonator z poprzeczną falą powierzchniową na krysztale tantalantu litu do zastosowań w czujnikach lepkości i temperatury cieczy		
Streszczenia wybranych publikacji pracowników ITME		25

# **STRESZCZENIA ARTYKUŁÓW ME 2016 - 44 - 3**

## **Optymalizacja procesu syntezy jednofazowych materiałów LiFePO<sub>4</sub> o nanometrycznych rozmiarach ziaren**

*ME 2016, 44, 3, s. 4*

Próbki materiału LiFePO<sub>4</sub> przygotowano zmodyfikowaną metodą zol - żel. Otrzymany ksorożel został roztarty w moździerzu i kalcynowany w piecu rurowym w atmosferze ochronnej, w przepływie azotu. Główny cel pracy jakim było obniżenie temperatury i czasu trwania procesu, zostało osiągnięty. Potwierdzono, że materiał ten składa się tylko z tryfilitowej fazy LiFePO<sub>4</sub>. Dowiedzono, że węgiel obecny w próbce, pochodzący z rozkładu pirolitycznego wyjściowych soli organicznych nie wpływa na formowanie się fazy krystalicznej.

## **Badanie metodami wysokorozdzielczej dyfraktometrii rentgenowskiej monokryształów ZnO bombardowanych jonami Ar**

*ME 2016, 44, 3, s. 9*

Z pomocą wysokorozdzielczej dyfraktometrii rentgenowskiej (HRXRD) badano tetragonalizację komórki elementarnej monokryształu tlenku cynku powstałą pod wpływem bombardowania jonami Ar. Objętościowe monokryształy ZnO o orientacji (00·1) były bombardowane jonami o energii 300 keV, w przedziale dawek od  $1 \times 10^{14} \text{ cm}^{-2}$  do  $4 \times 10^{16} \text{ cm}^{-2}$ . Zarejestrowano profile dyfrakcyjne otrzymywane metodą radialnego skanowania 2Teta/Omega, w otoczeniu węzła 00·4, sieci odwrotnej ZnO i w oparciu o założenia dynamicznej teorii dyfrakcji promieniowania rentgenowskiego w ujęciu Darwina, wykonano ich symulacje numeryczne. Na tej podstawie określono, w zależności od dawki, profil zmiany odległości płaszczyzn prostopadłych do osi c monokryształu ZnO. Stwierdzono, że dla niskich dawek, w ścisłe określonej objętości kryształu, powstaje dodatnie odkształcenie równoległe do osi c, wraz ze wzrostem dawki jonów to odkształcenie wzrasta, a po osiągnięciu pewnej krytycznej wartości ulega nasyceniu. To prowadzi do wniosku, że w implantowanej objętości kryształu powstaje wówczas odkształcenie plastyczne.

## **Rezonator z poprzeczną falą powierzchniową na krysztale tantalunu litu do zastosowań w czujnikach lepkości i temperatury cieczy**

*ME 2016, 44, 3, s. 17*

Celem pracy były obliczenia i pomiary parametrów poprzecznej akustycznej fali powierzchniowej w rezonatorze na kryształe tantalunu litu o orientacji 36°YX oraz pomiary lepkości i temperatury cieczy. Odpromienianie energii akustycznej od powierzchni do objętości kryształu zamodelowano wprowadzając współczynnik tlumienia fali różny od zera. Przyjęto najnowsze dostępne w literaturze stałe materiałowe tantalunu litu. Obliczono prędkość i współczynnik sprzężenia elektromechanicznego, współczynnik odbicia od pojedynczej elektrody, współczynnik tlumienia przy powierzchni swobodnej i metalizowanej oraz współczynnik anizotropii. Z wykorzystaniem rezonatora synchronicznego wykonano pomiary trzech pierwszych wielkości. Uzyskano dobrą zgodność pomiarów z obliczeniami. Skonstruowano dwukanałowy rezonator czuły na iloczyn lepkości i gęstości cieczy osadzonej na metalizowanej powierzchni międzyprzetwornikowej. Zbadano temperaturowy współczynnik częstotliwości (TWCz) kanału przeznaczonego do pomiaru temperatury.

# **THE ARTICLES ABSTRACTS ME 2016 - 44 - 3**

## **Optimization of synthesis of single phase nanostructured LiFePO<sub>4</sub> materials**

*ME 2016, 44, 3, p. 4*

LiFePO<sub>4</sub> samples were first prepared by a modified sol - gel process and then the resulting LiFePO<sub>4</sub> xerogel was ground and calcined in a tube furnace in an inert atmosphere in nitrogen flow. The main goal of this research work which was lowering the temperature and the time of synthesis of LiFePO<sub>4</sub> was achieved. It was confirmed that the material contains only a LiFePO<sub>4</sub> triphylite phase and that the presence of carbon resulting from pyrolysis of initial carbonaceous reagents does not affect the crystalline structure of the material.

## **HRXRD study of ZnO single crystals bombarded with Ar ions**

*ME 2016, 44, 3, p. 9*

High resolution X-ray diffraction methods (HRXRD) were used to study the tetragonalization of a unit cell in a zinc oxide single crystal resulting from the Ar-ion bombardment. Bulk ZnO (00·1) single crystals were bombarded with ions with the energy of 300 keV and a dose range between  $1 \times 10^{14} \text{ cm}^{-2}$  and  $4 \times 10^{16} \text{ cm}^{-2}$ . Diffraction profiles, obtained by radial 2Theta/Omega scans in the vicinity of the 00·4 ZnO reciprocal space node were measured and fitted to the curves calculated by means of a computer program based on the Darwin's dynamical theory of X-ray diffraction. On the basis of these numerical simulations, the profile of the interplanar spacing between planes perpendicular to the c axis of the ZnO single crystal were determined as a function of the Ar ion dose. It was found that positive deformation parallel to the c-axis appeared for the low doses in the bombarded crystal volume. When the dose is increased this deformation gets pronounced, and after reaching a certain critical value, it becomes saturated. This observation leads to the conclusion that the plastic deformation appears in the implanted volume of the crystal.

## **Resonator with transverse surface wave on lithium tantalate crystal for applications in viscosity and temperature sensors**

*ME 2016, 44, 3, p. 17*

The purpose of this work was to calculate and measure transverse surface acoustic wave resonators on 36°YX oriented lithium tantalate crystal as well as to measure of viscosity and temperature of liquids. An attenuation coefficient was used to model the leak of acoustic energy from surface into bulk of the crystal. The latest materials constants were used. Velocity, electromechanical coupling coefficient, reflection coefficient, attenuation coefficient under free and metallized surface, anisotropy coefficient were calculated, the first three of which were measured using synchronous resonator. A good agreement between measurements and calculations were obtained. Double-channel resonator was sensitive to viscosity and density multiplication product of liquid deposited on the metallized area between transducers. The temperature coefficient of frequency (TCF) of the temperature channel was measured.

## STRESZCZENIA WYBRANYCH PUBLIKACJI PRACOWNIKÓW ITME

### Numerical design of Metal-Organic Vapour Phase Epitaxy process for gallium nitride epitaxial growth

Skibinski J.<sup>1</sup>, Caban P.<sup>2</sup>, Wejrzanowski T.<sup>1</sup>, Oliver G.J.<sup>3</sup>, Kurzydlowski K.J.<sup>1</sup>

<sup>1</sup> Warsaw University of Technology, Faculty of Materials Science and Engineering Woloska 141, 02507 Warsaw, Poland

<sup>2</sup> Institute of Electronic Materials Technology, Wolczynska 133, 01919, Warsaw, Poland

<sup>3</sup> Cape Peninsula University of Technology, PO Box 1906, Bellville 7535, South Africa

*Crystal Research and Technology*, 2016, 51, 12, 762 - 770

The paper presents the results of numerical simulations and experimental measurements of the epitaxial growth of gallium nitride in Metal Organic Vapor Phase Epitaxy within a AIX-200/4RF-S reactor. The aim was to develop optimal process conditions for obtaining the most homogeneous crystal layer. Since there are many factors influencing the chemical reactions on the crystal growth area such as: temperature, pressure, gas composition or reactor geometry, it is difficult to design an optimal process. In this study various process pressures and hydrogen volumetric flow rates have been considered. Due to the fact that it is not economically viable to test every combination of possible process conditions experimentally, detailed 3D modeling has been used to get an overview of the influence of process parameters. Numerical simulations increased the understanding of the epitaxial process by calculating the heat and mass transfer distribution during the growth of gallium nitride. Appropriate chemical reactions were included in the numerical model which allowed for the calculation of the growth rate of the substrate. The results obtained have been applied to optimize homogeneity of GaN film thickness and its growth rate.

### High Q-Factor Millimeter-Wave Silicon Resonators

Krupka J.<sup>1</sup>, Kaminski P.<sup>2</sup>, Jensen L.<sup>3</sup>

<sup>1</sup> Warsaw Univ Technol, Inst Microelect & Optoelect, PL-00662 Warsaw, Poland

<sup>2</sup> Inst Elect Mat Technol, PL-01919 Warsaw, Poland

<sup>3</sup> Topsil Semicond Mat AS, DK-3600 Frederikssund, Denmark

*IEEE Transactions on Microwave Theory and Techniques*, 2016, 64, 12, 4149 - 4154

Resonators made of high-resistivity silicon (HRS) have been manufactured, and their characteristics were measured at a frequency range from 20 to 50 GHz. To study the influence of the material resistivity on Q-factor values, two HRSs were used. The first one was as-grown high-purity floating zone (FZ) silicon with a resistivity of  $\sim 70 \text{ k}\Omega \cdot \text{cm}$ . The second was FZ silicon irradiated with high-energy protons. The resistivity of the irradiated silicon was essentially the same as that of intrinsic silicon with a resistivity of  $\sim 400 \text{ k}\Omega \cdot \text{cm}$  at room temperature. Several whispering gallery modes were identified and measured on disk shape samples made on both materials. At room temperature and at a frequency of 50 GHz, the Q-factor values for the resonators made of the as-grown and the irradiated silicon are up to  $1.8 \times 10^4$  and up to  $6 \times 10^4$ , respectively.

### Ultrafast photocurrents at the surface of the three-dimensional topological insulator Bi<sub>2</sub>Se<sub>3</sub>

Braun L.<sup>1</sup>, Mussler G.<sup>2</sup>, Hruban A.<sup>3</sup>, Konczykowski M.<sup>4</sup>, Schumann T.<sup>5</sup>, Wolf M.<sup>1</sup>, Munzenberg M.<sup>5</sup>, Perfetti L.<sup>4</sup>, Kampfrath T.<sup>1</sup>

<sup>1</sup> Max Planck Gesell, Fritz Haber Inst, D-14195 Berlin, Germany

<sup>2</sup> Forschungszentrum Julich, PGI 9, D-52425 Julich, Germany

<sup>3</sup> Forschungszentrum Julich, JARA FIT, D-52425 Julich, Germany

<sup>4</sup> Inst Elect Mat Technol, PL-01919 Warsaw, Poland

<sup>5</sup> Univ Paris Saclay, CEA, CNRS, Lab Solides Irradiés, Ecole Polytech, F-91128 Palaiseau, France

<sup>6</sup> Ernst Moritz Arndt Univ Greifswald, Inst Phys, D-17489 Greifswald, Germany

*Nature Communications*, 2016, 7, 13259,

Three-dimensional topological insulators are fascinating materials with insulating bulk yet metallic surfaces that host highly mobile charge carriers with locked spin and momentum. Remarkably, surface currents with

tunable direction and magnitude can be launched with tailored light beams. To better understand the underlying mechanisms, the current dynamics need to be resolved on the timescale of elementary scattering events (similar to 10 fs). Here, we excite and measure photocurrents in the model topological insulator  $\text{Bi}_2\text{Se}_3$  with a time resolution of 20 fs by sampling the concomitantly emitted broadband terahertz (THz) electromagnetic field from 0.3 to 40 THz. Strikingly, the surface current response is dominated by an ultrafast charge transfer along the Se-Bi bonds. In contrast, photon-helicity-dependent photocurrents are found to be orders of magnitude smaller than expected from generation scenarios based on asymmetric depopulation of the Dirac cone. Our findings are of direct relevance for broadband optoelectronic devices based on topological-insulator surface currents.

## Negative Kerr Nonlinearity of Graphene as seen via Chirped-Pulse-Pumped Self-Phase Modulation

**Vermeulen N.<sup>1</sup>, Castello-Lurbe D.<sup>1</sup>, Cheng J.<sup>1,2</sup>, Pasternak I.<sup>3</sup>, Krajewska A.<sup>3</sup>, Ciuk T.<sup>3</sup>, Strupinski W.<sup>3</sup>, Thienpont H.<sup>1</sup>, Van Erps J.<sup>1</sup>**

<sup>1</sup> Brussels Photonics Team, Department of Applied Physics and Photonics, Vrije Universiteit Brussel, Pleinlaan 2, 1050 Brussel, Belgium

<sup>2</sup>Department of Physics, University of Toronto, 60 St. George Street, Toronto, Ontario M5S 1A7, Canada

<sup>3</sup> Institute of Electronic Materials Technology, Wolczynska 133, 01-919 Warsaw, Poland

*Physical Review Applied*, 2016, 6, 4, 044006

We experimentally demonstrate a negative Kerr nonlinearity for quasiundoped graphene. Hereto, we introduce the method of chirped-pulse-pumped self-phase modulation and apply it to graphene-covered silicon waveguides at telecom wavelengths. The extracted Kerr-nonlinear index for graphene equals  $n_{2,\text{gr}} = -10^{-13} \text{ m}^2/\text{W}$ . Whereas the sign of  $n_{2,\text{gr}}$  turns out to be negative in contrast to what has been assumed so far, its magnitude is in correspondence with that observed in earlier experiments. Graphene's negative Kerr nonlinearity strongly impacts how graphene should be exploited for enhancing the nonlinear response of photonic (integrated) devices exhibiting a positive nonlinearity. It also opens up the possibility of using graphene to annihilate unwanted nonlinear effects in such devices, to develop unexplored approaches for establishing Kerr processes, and to extend the scope of

the “periodic poling” method often used for second-order nonlinearities towards third-order Kerr processes. Because of the generic nature of the chirped-pulse-pumped self-phase modulation method, it will allow fully characterizing the Kerr nonlinearity of essentially any novel (2D) material.

## Toxicity of different forms of graphene in a chicken embryo model

**Szmidt M.<sup>1</sup>, Sawosz E.<sup>2</sup>, Urbańska K.<sup>1</sup>, Jaworski S.<sup>2</sup>, Kutwin M.<sup>2</sup>, Hotowy A.<sup>2</sup>, Wierzbicki M.<sup>2</sup>, Grodzik M.<sup>2</sup>, Lipińska L.<sup>3</sup>, Chwalibog A.<sup>4</sup>**

<sup>1</sup> Department of Morphological Sciences Warsaw University of Life Sciences, Warsaw, Poland

<sup>2</sup> Department of Animal Nutrition and Biotechnology Warsaw University of Life Sciences, Warsaw, Poland

<sup>3</sup> Institute of Electronic Materials Technology, Warsaw, Poland

<sup>4</sup> Department of Veterinary Clinical and Animal Sciences, University of Copenhagen, Frederiksberg Denmark

*Environmental Science and Pollution Research*, 2016, 23, 19, 19940 – 19948

In the present work, the toxicity of three forms of graphene: pristine graphene (pG), graphene oxide (GO), and reduced graphene oxide (rGO) was investigated using a chicken embryo model. Fertilized chicken eggs were divided into the control group and groups administered with pG, GO, and rGO, in concentrations of 50, 500, and 5000  $\mu\text{g}/\text{mL}$ . The experimental solutions were injected in ovo into the eggs, and at day 18 of incubation, the embryo survival, body and organ weights, the ultrastructure of liver samples, and the concentration of 8-hydroxy-2'-deoxyguanosine (8-OHdG) in the livers were measured. Survival of embryos decreased significantly after treatment with all types of graphene, but not in a dose-dependent manner. The body weights were only slightly affected by the highest doses of graphene, while the organ weights were not different among treatment groups. In all experimental groups, atypical hepatocyte ultrastructure and mitochondrial damage were observed. The concentration of the marker of DNA damage 8-OHdG in the liver significantly decreased after pG and rGO treatments. Further *in vivo* studies with different animal models are necessary to clarify the level of toxicity of different types of graphene and to estimate the concentrations appropriate to evaluate their biomedical applications and environmental hazard.

## STEM study of $\text{Li}_4\text{Ti}_5\text{O}_{12}$ anode material modified with Ag nanoparticles

Andrzejczuk M.<sup>1,5</sup>, Roguska A.<sup>2</sup>, Michalska M.<sup>3</sup>, Lipinska L.<sup>3</sup>, Czerwinski A.<sup>4</sup>, Cantoni M.<sup>5</sup>, Krawczynska A. T.<sup>1</sup>, Lewandowska M.<sup>1</sup>

<sup>1</sup> Faculty of Materials Science and Engineering, Warsaw University of Technology, Warsaw, Poland

<sup>2</sup> Institute of Physical Chemistry, Polish Academy of Sciences, Warsaw, Poland

<sup>3</sup> Institute of Electronic Materials Technology, Warsaw, Poland

<sup>4</sup> Faculty of Chemistry, University of Warsaw, Warsaw, Poland

<sup>5</sup> Ecole Polytechnique Federale de Lausanne, EPFL, CIME, Lausanne, Switzerland

Journal of Microscopy, 2016, 264, 1, 41 – 47

Comprehensive scanning transmission electron microscopy (STEM) analysis of  $\text{Li}_4\text{Ti}_5\text{O}_{12}$  (LTO) powder modified by deposited Ag nanoparticles was performed. Nanocomposite powders with Ag content of 1 wt.%, 4 wt.%, 10 wt.% were fabricated in a chemical process from suspensions of Ag and LTO. Apart from the STEM results, the presence of pure silver on the surface of the ceramic powder was confirmed by XRD and XPS analyses. The silver particles deposited on the LTO particles were characterized using the EDS mapping technique. The quantified results of the EDS mapping showed a relatively homogenous distribution of silver nanoparticles on the powder surface for every metal content. The mean diameter of the nanoparticles deposited on the LTO powder was about 4 nm in all cases. An increase in the Ag content during chemical surface modification did not cause changes in the microstructure. Focusing on an analysis of the metallic nanoparticles on the ceramic powder, electron tomography was used as an investigative technique. A very precise analysis of three-dimensional nanostructures is desirable for a comprehensive analysis of complex materials. The quantified analysis of the Ag nanoparticles visualized using electron tomography confirmed the results of the size measurements taken from the two-dimensional EDS maps.

## Roadmap on optical metamaterials

Urbas A. M.<sup>1</sup>, Jacob Z.<sup>2,3</sup>, Dal Negro L.<sup>4</sup>, Engheta N.<sup>5</sup>, Boardman A. D.<sup>6</sup>, Egan P.<sup>6</sup>, Khanikaev A. B.<sup>7</sup>, Menon V.<sup>8</sup>, Ferrera M.<sup>3,9</sup>, Kinsey N.<sup>3</sup>, DeVault C.<sup>3</sup>, Kim J.<sup>3</sup>, Shalaev V.<sup>3</sup>, Boltasseva A.<sup>3</sup>, (...) Pawlak, D. A.<sup>20,21</sup>, ...

<sup>1</sup> Materials and Manufacturing Directorate, Air Force Research

Laboratory, Wright Patterson Air Force, Base, Ohio 45433, USA

<sup>2</sup> Department of Electrical and Computer Engineering, University of Alberta, Edmonton, AB T6G 2V4, Canada

<sup>3</sup> Birck Nanotechnology Center, School of Electrical and Computer Engineering, Purdue University, West Lafayette, IN 47906, USA

<sup>4</sup> Department of Electrical and Computer Engineering & Photonics Center, and Division of Materials Science and Engineering, Boston University, 8 Saint Mary Street, Boston, Massachusetts 02215, USA

<sup>5</sup> Department of Electrical and Systems Engineering, University of Pennsylvania, Philadelphia, PA 19104, USA

<sup>6</sup> Joule Physics Laboratory, Institute for Materials Research, University of Salford, Manchester, M5 4WT, UK

<sup>7</sup> Queens College and The Graduate Center of The City University of New York, Queens, New York 11367, USA

<sup>8</sup> City College and The Graduate Center of The City University of New York, New York, New York 10031, USA

<sup>9</sup> School of Engineering and Physical Sciences, Heriot-Watt University, David Brewster Building, Edinburgh, Scotland EH14 4AS, UK

<sup>20</sup> Institute of Electronic Materials Technology, ul. Wolczynska 133, 01-919 Warsaw, Poland

<sup>21</sup> Centre of New Technologies University of Warsaw, ul. Banacha 2C, 02-097 Warsaw, Poland

Journal of Optics, 2016, 18, 9, 093005, 53pp

Optical metamaterials have redefined how we understand light in notable ways: from strong response to optical magnetic fields, negative refraction, fast and slow light propagation in zero index and trapping structures, to flat, thin and perfect lenses. Many rules of thumb regarding optics, such as  $\mu = 1$ , now have an exception, and basic formulas, such as the Fresnel equations, have been expanded. The field of metamaterials has developed strongly over the past two decades. Leveraging structured materials systems to generate tailored response to a stimulus, it has grown to encompass research in optics, electromagnetics, acoustics and, increasingly, novel hybrid material responses. This roadmap is an effort to present emerging fronts in areas of optical metamaterials that could contribute and apply to other research communities. By anchoring each contribution in current work and prospectively discussing future potential and directions, the authors are translating the work of the

field in selected areas to a wider community and offering an incentive for outside researchers to engage our community where solid links do not already exist.

## Stopping and straggling of H and He in ZnO

**Fadanelli R. C.<sup>1</sup>, Nascimento, C. D.<sup>1</sup>, Montanari C. C.<sup>2,3</sup>, Aguiar J. C.<sup>4</sup>, Mitnik D.<sup>2,3</sup>, Turos A.<sup>5,6</sup>, Guziewicz E.<sup>7</sup>, Behar M.<sup>1</sup>**

<sup>1</sup> Laboratorio de Implantação Iônica, Instituto de Física, Universidade Federal do Rio Grande do Sul Porto Alegre Brazil

<sup>2</sup> Instituto de Astronomía y Física del Espacio (CONICET-UBA), and Departamento de Física, Facultad de Ciencias Exactas y Naturales, Universidad de Buenos Aires, Buenos Aires, Argentina

<sup>3</sup> Autoridad Regulatoria Nuclear, Av. Libertador 8250, C1429BNP, Buenos Aires Argentina

<sup>4</sup> Institute of Electronic Materials Technology, Warsaw, Poland

<sup>5</sup> National Centre for Nuclear Research, Soltana 7, Otwock, Poland

<sup>6</sup> Institute of Physics, Polish Academy of Sciences, Warsaw, Poland

*The European Physical Journal D*, 2016, 70, 9, 178

We present experimental and theoretical values for the energy loss of H and He ions in Zinc oxide, in mean value (stopping per unit path length) and mean square value (energy loss straggling). The measurements were carried out using the Rutherford Backscattering technique for (300–2000) keV H ions and (300–5000) keV He ions. Present experimental data are the first set of stopping and straggling values in this oxide. The theoretical research was encouraged considering the molecular description of ZnO as crystal solid using the density functional theory. The energy loss calculations for H and He ions with different charge states were performed with the shelwise local plasma approximation (SLPA). The molecular versus the Bragg-rule description is also discussed. The equilibrium charge state of He inside ZnO is analyzed based on the present stopping measurements, and a semiempirical charge state distribution is proposed. Present experimental and theoretical values show good agreement for both the stopping and the straggling. We also compare our data with the SRIM2013 and with CasP5.2 values.

## Optical and X-Ray Topographic Studies of Dislocations, Growth-Sector Boundaries, and Stacking Faults in Synthetic Diamonds

**Moore M.<sup>1</sup>, Nailer S. G.<sup>2</sup>, Wierzchowski W. K.<sup>3</sup>**

<sup>1</sup> Department of Physics, Royal Holloway University of London, Surrey, TW20 0EX Egham, UK

<sup>2</sup> Hilti Corporation, Feldkircherstrasse 100, 9494 Schaan, Liechtenstein

<sup>3</sup> The Institute of Electronic Materials Technology, 133, 01-919 Warsaw Wólczyńska, Poland

*Crystals*, 2016, 6, 7, 71

The characterization of growth features and defects in various high-pressure high-temperature (HPHT) synthetic diamonds has been achieved with optical and X-ray topographic techniques. For the X-ray studies, both characteristic and synchrotron radiation were used. The defects include dislocations, stacking faults, growth banding, growth sector boundaries, and metal inclusions. The directions of the Burgers vectors of many dislocations (edge, screw, and mixed 30 degrees, 60 degrees, and 73.2 degrees), and the fault vectors of stacking faults, were determined as  $<110>$  and  $1/3 <111>$  respectively. Some dislocations were generated at metallic inclusions; and some dislocations split with the formation of stacking faults.

## Aqueous biological graphene based formulations for ink-jet printing

**Dybowska-Sarapuk Ł.<sup>1,5</sup>, Rumiński S.<sup>2,3,4</sup>, Wróblewski G.<sup>1</sup>, Śloma M.<sup>1</sup>, Młożniak A.<sup>5</sup>, Kalaszczyńska I.<sup>2,3</sup>, Lewandowska-Szumiel M.<sup>2,3</sup>, Jakubowska M.<sup>1,5</sup>**

<sup>1</sup> Warsaw University of Technology, Faculty of Mechatronics, Andrzeja Boboli 8, 02-525 Warsaw, Poland

<sup>2</sup> Medical University of Warsaw, Department of Histology and Embryology, Centre for Biostructure Research, Chałubińskiego 5, 02-004 Warsaw, Poland

<sup>3</sup> Centre for Preclinical Research and Technology, Banacha 1B, 02-097 Warsaw, Poland

<sup>4</sup> Postgraduate School of Molecular Medicine, Żwirki i Wigury 61, 02-091 Warsaw, Poland

<sup>5</sup> Institute of Electronic Materials Technology, Wólczyńska 133, 01-919 Warsaw, Poland

*Polish Journal of Chemical Technology*, 2016, 18, 2, 46 - 52

The aim of the study was to produce heterophasic graphene nanoplatelets based formulation designed for ink-jet printing and biomedical applications. The compositions should meet two conditions: should be cytocompatible and have the rheological properties that allow to apply it with ink-jet printing technique. In view of the above conditions, the selection of suspensions components, such as binder, solvent and surfactants was performed. In the first stage of the research the homogeneity of the dispersion of nanoplatelets and their sedimentation behaviour in diverse solutions were tested. Subsequently, the cytotoxicity of each ink on human mesenchymal stem cells was examined using the Alamar Blue Test. At the same time the rheology of the resulting suspensions was tested. As a result of these tests the best ink composition was elaborated: water, polyethylene glycol, graphene nanoplatelets and the surfactant from DuPont company.

### **Development of x-ray and ion diagnostics of plasma obtained with a 10-TW femtosecond laser**

**Ryć L.<sup>1</sup>, Dobrzański L.<sup>2</sup>, Dubecky F.<sup>3</sup>, Jabłoński S.<sup>1</sup>, Parys P.<sup>1</sup>, Slysz W.<sup>4</sup>, Rosiński M.<sup>1</sup>**

<sup>1</sup> Institute of Plasma Physics and Laser Microfusion, EURATOM Association, Warsaw, Poland

<sup>2</sup> Institute of Electronic Materials Technology, Warsaw, Poland

<sup>3</sup> Institute of Electrical Engineering, Slovak Academy of Sciences, Bratislava, Slovak Republic

<sup>4</sup> Institute of Electron Technology, Warsaw, Poland

*Physica Scripta*, 2016, 91, 7, 074008

Several x-ray and ion semiconductor detectors have been developed for the diagnostics of femtosecond laser plasma generated by a 10-TW laser which was recently commissioned for operation at the Institute of Plasma Physics and Laser Microfusion, Warsaw. A range of detectors has been employed including a CdTe detector for hard x-rays and four detectors for proton detection. These four are SiC and GaN employing a sandwich structure, an interdigitated M-S-M InP detector and finally a silicon photo-diode equipped with an aluminium filter (to shield against scattered light). The detectors presented are innovative as they are not commonly used for the diagnostic of laser plasma. The details of the internal structures of the detectors are presented. The immunity of the detectors to the noise coming from the laser system and the femtosecond plasma is discussed. Lastly, the

possibility for further modifications and improvements are considered and discussed.

### **Characterisation of graphene-based layers for dye-sensitised solar cells application**

**Lukaszkowicz K.<sup>1</sup>, Pawlyta M.<sup>1</sup>, Pasternak I.<sup>2</sup>, Dobrzański L. A.<sup>1</sup>, Prokopowicz M.<sup>1</sup>, Szindler M.<sup>1</sup>, Drygala A.<sup>1</sup>, Sitek J.<sup>1,2</sup>**

<sup>1</sup> Silesian Tech. Univ., Inst Engn Mat & Biomat, Konarskiego 18A, PL-44100 Gliwice, Poland

<sup>2</sup> Inst. Elect. Mat. Technol., Wolczynska 133, PL-01919 Warsaw, Poland

*Surface Engineering*, 2016, 32, 11, 816-822

The influence of the graphene-based counter electrode on the structure, optical properties and electrocatalytic activity of dye-sensitised solar cells (DSCC) was analysed. The graphene and reduced graphene oxide were deposited by CVD and spin-coating method on the FTO glass substrate, respectively. HRTEM investigation confirms the crystallographic structure of graphene. The investigated layers show flat transmittance spectra across the visible and near-infrared region. The charge transfer resistance of the graphene-based film was analysed by electrochemical impedance measurement. The obtained results show the possibility of replacing expensive platinum in DSCC by using graphene-based counter electrode.

### **InP nanowires quality control using SEM and Raman spectroscopy**

**Grodecki K.<sup>1</sup>, Dumiszewska E.<sup>2</sup>, Romaniec M.<sup>2</sup>, Strupinski W.<sup>2</sup>**

<sup>1</sup> Military University of Technology, 2 Kaliskiego St., 00-908 Warsaw, Poland

<sup>2</sup> Institute of Electronic Materials Technology, 133 Wolczynska Str., 01-919 Warsaw, Poland

*Materials Science-Poland*, 2016, 34, 4, 851 - 855

Three different types of samples of InP nanowires, i.e. undoped, doped with Si and doped with Te, were grown and measured using SEM and Raman spectroscopy. Scanning Electron Microscope (SEM) images showed differences in the length, homogeneity and curvature of the nanowires. The most homogenous wires, grown most perpendicular to the surface, were those Si doped. They were also the shortest. Raman spectroscopy showed that the nanowires doped with

Si had the lowest Full Width at Half Maximum (FWHM) TO band, which suggests the highest crystal quality of these wires. For the wires doped with Te, which were the most inhomogeneous, a low energy acoustic band was also observed, which suggests the lowest crystal quality of these structures.

## **Optical properties of transparent electrodes based on carbon nanotubes and graphene platelets**

**Wroblewski G.<sup>1</sup>, Swatowska B.<sup>2</sup>, Dybowska-Sarapuk L.<sup>1</sup>, Jakubowska M.<sup>1,3</sup>, Stapiński T.<sup>2</sup>**

<sup>1</sup> Institute of Metrology and Biomedical Engineering Warsaw University of Technology, Warsaw, Poland

<sup>2</sup> AGH University of Science and Technology, Kraków, Poland

<sup>3</sup> Institute of Electronic Materials Technology, Warsaw, Poland

*Journal of Materials Science: Materials in Electronics*, 2016, 27, 12, 12764 - 12771

Composite transparent electrodes based on carbon nanostructures such as multiwalled carbon nanotubes and graphene platelets were spray coated onto glass substrates and characterized by spectrophotometry and spectroscopic ellipsometry measurements. The dispersion relations of the ellipsometric angle rate, i.e. I<spacing diaeresis> and Delta versus wavelength lambda were measured in spectral range from 190 to 1700 nm. On the basis of these results, it was possible to estimate the value of the refractive index and extinction coefficient. Effective medium approximation model was chosen to calculate the optical constants of a mixed material. The average surface roughness and the average thickness of spray coated transparent resistive layers were also determined. The materials have a heterogeneous structure as confirmed by scanning electron microscopy and optical measurements (changes of depolarisation). From the Tauc plot it was possible to determine the energy gap. The influence of the coating process and the paint preparation on the optical properties was observed.

## **Impact of Different Conditions of Technological Process on Thermoelectric Properties of Fine-Grained PbTe**

**Krolicka A.<sup>1</sup>, Materna A.<sup>1</sup>, Piersa M.<sup>1</sup>, Mirowska A.<sup>1</sup>**

<sup>1</sup> Institute of Electronic Materials Technology, Wólczyńska 133, 01-919 Warsaw, Poland

*Acta Physica Polonica A*, 2016, 130, 5, 1255 - 1258

The aim of this work was to obtain PbTe material in the desired way in order to control the combined impact of lattice disorder, nanoscale precipitates and reduced grain sizes on the thermoelectric properties of this material. To achieve this, PbTe ingot doped with Ag was obtained by the Bridgman method, followed by ball-milling, cold pressing and sintering. In order to estimate crystallites diameters grain size measurements were carried out using the optical microscopy. Studies of electrical and thermoelectric properties of fine-grained material were performed. In order to analyze the morphology and the composition scanning electron microscopy and energy-dispersive X-ray spectroscopy were performed. Energy-dispersive X-ray spectroscopy analysis also revealed presence of Ag-Te precipitates.

## **Effects of Carbon Allotropic Forms on Microstructure and Thermal Properties of Cu-C Composites Produced by SPS**

**Pietrzak K.<sup>1</sup>, Sobczak N.<sup>2</sup>, Chmielewski M.<sup>1</sup>, Homa M.<sup>2</sup>, Gazda, A.<sup>2</sup>, Zybal R.<sup>3</sup>, Strojny-Nedza A.<sup>1</sup>**

<sup>1</sup> Institute of Electronic Materials Technology, Warsaw, Poland

<sup>2</sup> Foundry Research Institute, Kraków, Poland

<sup>3</sup> Faculty of Materials Science Engineering Warsaw University of Technology, Warsaw, Poland

*Journal of Materials Engineering and Performance*, 2016, 25, 8, 3077 – 3083

Combination of extreme service conditions and complex thermomechanical loadings, e.g., in electronics or power industry, requires using advanced materials with unique properties. Dissipation of heat generated during the operation of high-power electronic elements is crucial from the point of view of their efficiency. Good cooling conditions can be guaranteed, for instance, with materials of very high thermal conductivity and low thermal expansion coefficient, and by designing the heat dissipation system in an accurate manner. Conventional materials such as silver, copper, or their alloys, often fail to meet such severe requirements. This paper discusses the results of investigations connected with Cu-C (multiwall carbon nanotubes (MWNTs), graphene nanopowder (GNP), or thermally reduced graphene oxide (RGO)) composites, produced using the spark plasma sintering technique. The obtained composites are characterized by uniform distribution of a carbon phase and high relative density. Compared with pure copper, developed

materials are characterized by similar thermal conductivity and much lower values of thermal expansion coefficient. The most promising materials to use as heat dissipation elements seems to be copper-based composites reinforced by carbon nanotubes (CNTs) and GNP.

### **The Influence of $\text{Al}_2\text{O}_3$ Powder Morphology on the Properties of Cu-Al<sub>2</sub>O<sub>3</sub> Composites Designed for Functionally Graded Materials (FGM)**

**Strojny-Nedza A.<sup>1</sup>, Pietrzak K.<sup>1</sup>, Weglewski W.<sup>2</sup>**

<sup>1</sup> Institute of Electronic Materials Technology, Warsaw, Poland

<sup>2</sup> Institute of Fundamental Technological Research, Warsaw, Poland

*Journal of Materials Engineering and Performance*, 2016, 25, 8, 3173 – 3184

In order to meet the requirements of an increased efficiency applying to modern devices and in more general terms science and technology, it is necessary to develop new materials. Combining various types of materials (such as metals and ceramics) and developing composite materials seem to be suitable solutions. One of the most interesting materials includes Cu-Al<sub>2</sub>O<sub>3</sub> composite and gradient materials (FGMs). Due to their potential properties, copper-alumina composites could be used in aerospace industry as rocket thrusters and components in aircraft engines. The main challenge posed by copper matrix composites reinforced by aluminum oxide particles is obtaining the uniform structure with no residual porosity (existing within the area of the ceramic phase). In the present paper, Cu-Al<sub>2</sub>O<sub>3</sub> composites (also in a gradient form) with 1, 3, and 5 vol.% of aluminum oxide were fabricated by the hot pressing and spark plasma sintering methods. Two forms of aluminum oxide ( $\alpha\text{Al}_2\text{O}_3$  powder and electrocorundum) were used as a reinforcement. Microstructural investigations revealed that near fully dense materials with low porosity and a clear interface between the metal matrix and ceramics were obtained in the case of the SPS method. In this paper, the properties (mechanical, thermal, and tribological) of composite materials were also collected and compared. Technological tests were preceded by finite element method analyses of thermal stresses generated in the gradient structure, and additionally, the role of porosity in the formation process of composite properties was modeled. Based on the said modeling, technological conditions for obtaining FGMs were proposed.

### **The Influence of the Particle Size on the Adhesion Between Ceramic Particles and Metal Matrix in MMC Composites**

**Jarzabek D. M.<sup>1</sup>, Chmielewski M.<sup>2</sup>, Dulnik J.<sup>1</sup>, Strojny-Nedza A.<sup>2</sup>**

<sup>1</sup> Institute of Fundamental Technological Research, Warsaw, Poland

<sup>2</sup> Institute of Electronic Materials Technology, Warsaw, Poland

*Journal of Materials Engineering and Performance*, 2016, 25, 8, 3139 – 3145

This study investigated the influence of the particle size on the adhesion force between ceramic particles and metal matrix in ceramic-reinforced metal matrix composites. The Cu-Al<sub>2</sub>O<sub>3</sub> composites with 5 vol.% of ceramic phase were prepared by a powder metallurgy process. Alumina oxide powder as an electrocorundum ( $\text{Al}_2\text{O}_3$ ) powder with different particle sizes, i.e., fine powder < 3  $\mu\text{m}$  and coarse powder of 180  $\mu\text{m}$  was used as a reinforcement. Microstructural investigations included analyses using scanning electron microscopy with an integrated EDS microanalysis system and transmission microscopy. In order to measure the adhesion force (interface strength), we prepared the microwires made of the investigated materials and carried out the experiments with the use of the self-made tensile tester. We have observed that the interface strength is higher for the sample with coarse particles and is equal to  $74 \pm 4$  MPa and it is equal to  $68 \pm 3$  MPa for the sample with fine ceramic particles.

### **Extending of flat normal dispersion profile in all-solid soft glass nonlinear photonic crystal fibres**

**Siwicki B.<sup>1,2</sup>, Kasztelanic R.<sup>1,2</sup>, Klimczak M.<sup>1</sup>, Cimek J.<sup>1,2</sup>, Pysz D.<sup>1</sup>, Stepien R.<sup>1</sup>, Buczynski R.<sup>1,2</sup>**

<sup>1</sup> Institute of Electronic Materials Technology, Glass Department, Wólczyńska 133, 01-919 Warsaw, Poland

<sup>2</sup> University of Warsaw, Faculty of Physics, Pasteura 7, 02-093 Warsaw, Poland

*Journal of Optics*, 2016, 8, 6, 065102

The bandwidth of coherent supercontinuum generated in optical fibres is strongly determined by the all-normal dispersion characteristic of the fibre. We investigate all-normal dispersion limitations in all-solid oxide-based soft glass photonic crystal fibres with various relative inclusion sizes and lattice constants. The influence of material

dispersion on fibre dispersion characteristics for a selected pair of glasses is also examined. A relation between the material dispersion of the glasses and the fibre dispersion has been described. We determined the parameters which limit the maximum range of flattened all-normal dispersion profile achievable for the considered pair of heavy-metal-oxide soft glasses.

## Rheology of inks for various techniques of printed electronics

**Dybowska-Sarapuk L.<sup>1</sup>, 2, Szalapak J.<sup>1</sup>, Wróblewski G.<sup>1</sup>, Wyżkiewicz I.<sup>1</sup>, Słoma M.<sup>1,2</sup>, Jakubowska M.<sup>1,2</sup>**

<sup>1</sup> Institute of Electronic Materials Technology, Warsaw, Poland

<sup>2</sup> Faculty of Mechatronics Warsaw University of Technology, Warsaw, Poland

*Advanced Mechatronics Solutions*, 2016, 393, 447 - 451

The inks and pastes with carbon nanoparticles, such as graphene nanoplatelets and carbon nanotubes, for diverse printed electronics techniques were produced. These composite materials, dedicated for screen printing, inkjet printing, spray coating and gravure printing were tested in context of their rheological properties. After comparing the obtained values of viscosity with standard values found in literature, it was confirmed that the tested suspensions may meet rheological requirements of particular techniques and can be transferred correctly on the substrate in the form of good quality pattern.

## Assessment of Graphene Coatings Influence on Tribological Properties of Surfaces

**Missala T.<sup>1</sup>, Szewczyk R.<sup>1</sup>, Winiarski W.<sup>1</sup>, Hamela M.<sup>1</sup>, Kaminski M.<sup>1</sup>, Jus A.<sup>1</sup>, Tomaszik J.<sup>2</sup>, Nowicki M.<sup>2</sup>, Pasternak I.<sup>3</sup>**

<sup>1</sup> Industrial Research Institute for Automation and Measurements PIAP, Warsaw Poland

<sup>2</sup> Institute of Metrology and Biomedical Engineering Warsaw University of Technology Warsaw, Poland

<sup>3</sup> Institute of Electronic Materials Technology, Warsaw Poland

*Advances in Intelligent Systems and Computing*, 2016, 440, 781 - 788

This paper presents results of experiments carried out to determine influence of graphene coating on tribological

properties of surfaces of friction pairs. Within these experiments series of 24 h tribological tests of sliding friction between examined surfaces on specially designed measuring stand were conducted. Subject of study in these tests were electrolytic copper plated steel samples, additionally covered with graphene and, as a reference, identically prepared samples without the graphene layer. As a result of these experiments characteristics of coefficient of friction and temperature between surfaces, as well as changes in mass and roughness before and after tests were obtained. Based on these results improvement of tribological properties of sliding surfaces was shown.

## Early stages of irradiation induced dislocations in urania

**Chartier A.<sup>1</sup>, Onofri C.<sup>2</sup>, Van Brutzel L.<sup>1</sup>, Sabathier C.<sup>2</sup>, Dorosh O.<sup>3</sup>, Jagielski J.<sup>3,4</sup>**

<sup>1</sup> DEN, Service de Corrosion et du Comportement des Matériaux dans leur Environnement, CEA, Université Paris-Saclay, F-91191 Gif-Sur-Yvette, France

<sup>2</sup> DEN, Service d'Etudes et de Simulation du Comportement des Combustibles, CEA, F-13108 Saint Paul-lez-Durance, France

<sup>3</sup> National Center for Nuclear Research, 05-400 Swierk/Otwock, Poland

<sup>4</sup> Institute of Electronic Materials Technology, Wolczynska 133, 01-919 Warsaw, Poland

*Appl. Phys. Lett.*, 2016, 109, 181902

The early stages of nucleation and growth of dislocations by irradiation in urania is clarified based on the combination of experiments and atomistic calculations. It is established that irradiation induced dislocations follow a five stage process: (i) point defects are first created by irradiation, (ii) they aggregate into clusters, (iii) from which nucleate Frank loops, (iv) which transform into unfaulted loops via Shockley that in turn grow, and (v) finally reorganize into forest dislocations. Stages (i)-(iii) participate in the lattice expansion while the onset of lattice contraction starts with stage (iv), i.e., when unfaulted loops nucleate. Irradiation induced dislocations operate in the spontaneous recombination regime, to be opposed to the thermal diffusion regime. Body of arguments collaborates to this statement, the main one is the comparison between characteristic distances estimated from the dose rate ( $V\text{-at}/(K_0 \times \tau)$ ) $(1/3)$  and from the diffusion coefficient ( $D \times \tau$ ) $(1/2)$ . Such a comparison identifies materials under irradiation as belonging either into the recombination regime or not. Published by AIP Publishing.

## **Wskazówki dla autorów**

Redakcja wydawnictwa **Materiały Elektroniczne** prosi autorów o nadsyłanie zamówionych artykułów pocztą elektroniczną, pod adres **ointe@itme.edu.pl** lub na nośniku magnetycznym, według następujących specyfikacji:

### **Tekst**

- a) Treść artykułu powinna być dostarczona w plikach o rozszerzeniu obsługiwany przez program Word (najlepiej DOC i DOCX). Tekst powinien być pisany w sposób ciągły, podzielony na kolejno ponumerowane, zawierające tytuły, rozdziały. Oznaczenia zmiennych należy pisać czcionką pochyłą (kursywą). W tekście powinny być zaznaczone miejsca, w których mają znajdować się materiały ilustracyjne, jednak same grafiki powinny być umieszczone poza nim w oddzielnych plikach (patrz punkt 4).
- b) Podpisy do rysunków w języku polskim i angielskim, również winny być zapisane w oddzielnym pliku.
- c) Na pierwszej stronie artykułu powinny znajdować się następujące elementy: imię i nazwisko autora, tytuł naukowy, nazwa miejsca pracy, adres pocztowy, e-mail, tytuł artykułu zarówno w języku polskim jak i angielskim.

### **Streszczenie**

- a) Do artykułu należy dołączyć streszczenie w języku polskim i angielskim. Każde z nich nie powinno przekraczać 200 słów.
- b) Należy także dodać słowa kluczowe zarówno w języku polskim jak i angielskim.

### **Bibliografia**

a) Pozycje bibliograficzne należy podawać w nawiasach kwadratowych w kolejności ich występowania.

b) Sposoby sporządzania opisów bibliograficznych:

- Opis bibliograficzny całej książki:

Autor: Tytuł. Numer wydania. Miejsce wydania: Nazwa wydawca, Rok wydania, ISBN.

- Opis bibliograficzny pracy zbiorowej pod redakcją:

Tytuł. Pod red. (nazwiska redaktorów): Numer wydania. Miejsce wydania: Nazwa wydawca, Rok wydania, ISBN.

- Opis bibliograficzny fragmentu (rozdziału) książki, (gdy cała książka jest tego samego autorstwa):

Autor: Tytuł książki. Numer wydania. Miejsce wydania: Nazwa wydawca, Rok wydania, ISBN. Tytuł fragmentu, Strony rozdziału.

- Opis bibliograficzny fragmentu (rozdziału) książki z pracy zbiorowej:

Autor: Tytuł fragmentu. W: Tytuł książki. Miejsce wydania: Nazwa wydawca, Rok wydania, ISBN.

- Opis bibliograficzny artykułu z czasopisma:

Autor: Tytuł artykułu . „Tytuł czasopisma” Rok, Wolumen, Numer, Strony.

- Opis artykułu w czasopiśmie internetowym:

Autor: Tytuł artykułu [on line], Rok, Wolumen, Numer [dostęp – data] Strony, Adres w Internecie. ISSN

- Strona WWW:

Autor: Tytuł [on line]. Miejsce wydania: Instytucja sprawcza [dostęp – data], Adres w internecie.

### **Elementy graficzne**

- a) Każdy materiał ilustracyjny powinien być zapisany w oddzielnym pliku (PCX, TIF, BMP, WFM, WPG, JPG) o rozdzielcości nie mniejszej niż 150 dpi.
- b) W przypadku materiałów ilustracyjnych niebędących oryginalnym dorobkiem autora/ów należy zacytować ich źródło, umieszczając je w bibliografii.

### **Wzory**

a) Wzory należy numerować kolejno cyframi arabskimi

b) Zmienne należy oznaczyć czcionką pochyłą.

c) W przypadku wzorów niebędących oryginalnym dorobkiem autora/ów należy zacytować ich źródło, umieszczając je w bibliografii.

**Autora obowiązuje wykonanie korekty autorskiej.**



# INSTYTUT TECHNOLOGII MATERIAŁÓW ELEKTRONICZNYCH

ul. Wólczyńska 133, 01-919 Warszawa

tel.: (+48 22) 835 30 41

e-mail: [itme@itme.edu.pl](mailto:itme@itme.edu.pl)

[www.itme.edu.pl](http://www.itme.edu.pl)

Instytut Technologii Materiałów Elektronicznych jest wiodącym polskim ośrodkiem prowadzącym badania naukowe oraz prace badawczo-rozwojowe w zakresie fizyki ciała stałego, projektowania i technologii nowoczesnych materiałów, struktur i podzespołów dla mikro- i nano-elektroniki, fotoniki i inżynierii.

Badania te dotyczą następujących grup materiałów i ich zastosowań w postaci podzespołów:

- **materiały nowej generacji:** grafen, metamaterialy, materiały samoorganizujące się i gradienutowe, nanokryształy tlenkowe w różnych matrycach (szkło, tworzywa sztuczna);
- **materiały półprzewodnikowe i ich zastosowania:**
  - monokryształy hodowane metodą Czochralskiego Si, GaAs, GaP, GaSb, InAs, InSb, InP i transportu z fazy gazowej SiC, o średnicach do 10 cm;
  - warstwy epitaksjalne półprzewodnikowe uzyskiwane za pomocą metod CVO i MOCVD z Si, SiC, GaN, AlN, InN, GaAs, GaP, GaSb, InP, InSb oraz opartych o nie związków potrójnych i poczwórnnych;
  - podzespoły dla elektroniki i fotoniki: diody Schottky'ego, tranzystory FET i HEMT, lasery, fotodetektory, IR i UV;
- **materiały tlenkowe i ich zastosowania:**
  - monokryształy, YAG domieszkowany: (Nd, Yb, Er, Pr, Ho, Tm, Cr), YVO<sub>3</sub>: (Nd, Tm, Ho, Er, Pr) i podwójnie domieszkowany: (Ho + Yb, Er + Yb), GdVO<sub>4</sub>: (Er, Tm); LuVO<sub>4</sub>: (Er, Tm); GdCoB: (Nd, Yb) dla zastosowań laserowych; kwarc, LiNbO<sub>3</sub>, LiTaO<sub>3</sub>, SeBa<sub>(1-x)</sub>O<sub>6</sub> dla zastosowań elektrooptycznych i piezoelektrycznych; CaF<sub>2</sub>, BaF<sub>2</sub>, jako materiały przezroczyste; Ca<sub>4</sub>GdO(BO)<sub>3</sub> jako materiał nieliniowy oraz NdGaO<sub>3</sub>, SrLaGaO<sub>4</sub>, SrLaAlO<sub>4</sub>, jako materiały podłożowe dla osadzania warstw nadprzewodników wysokotemperaturowych;
  - szkła o zadanych charakterystykach spektralnych i szkła aktywne;
  - ceramiki (Al<sub>2</sub>O<sub>3</sub>, Y<sub>2</sub>O<sub>3</sub>, ZrO<sub>2</sub>, Si<sub>3</sub>N<sub>4</sub>), ceramiki przezroczyste i aktywne;
  - Warstwy epitaksjalne YAG: Nd, Cr dla zastosowań laserowych;
  - światłowody specjalne, fotoniczne, aktywne i obrazowody;
  - podzespoły dla elektroniki i fotoniki: filtry i rezonatory z akustyczną falą powierzchniową; soczewki dyfrakcyjne, maski chromowe do fotolitografii;
- **inne materiały dla elektroniki:**
  - kompozyty metalowo-ceramiczne, kompozyty metalowe;
  - złącza zaawansowanych materiałów ceramicznych (Si<sub>3</sub>N<sub>4</sub>, AlN), kompozytów ceramiczno-metalowych i ceramik z metalami;
  - metale czyste (Ga, In, Al, Cu, Zn, Ag, Sb);
  - pasty do układów hybrydowych;
  - materiały dla jonowych ogniw litowych, ogniw paliwowych i kondensatorów.

Instytut prowadzi również badania i wykonuje usługi w zakresie:

- **innych technologii HI-TECH:** fotolitografia, elektronolitografia, osadzanie cienkich warstw, trawienie, obróbka termiczna;
- **charakteryzacji materiałów:** spektrometria mas i Mössbauer, elektronowy rezonans paramagnetyczny (EPR), rozpraszanie wsteczne Rutheforda (RBS), absorpcja atomowa, wysokorozdzielcza dyfrakcja rentgenowska, spektroskopia optyczna i w podczerwieni (FTIR), pomiary widm promieniowania, fotoluminescencja, mikroskopia optyczna i skaningowa mikroskopia elektronowa i sił atomowych (AFM); spektroskopia głębkowych poziomów: pojemnościowa (DLTS) i fotoprądowa (PITS), pomiary impedancyjne i szumów, temperaturowa analiza fazowa, pomiary dyfuzyjności ciepła.